A 585 GHz Diffusion-Cooled Niobium Hot-Electron Bolometric Mixer Element for Imaging Applications

Lei Liu, Robert M. Weikle, II, Arthur W. Lichtenberger, Acar Isin, and Bascom S. Deaver, Jr.

Abstract—Two prototype silicon-supported niobium hot-electron bolometric (HEB) mixers have been designed and fabricated for operation at 585 GHz. The HEB's are integrated into annular slot antennas that incorporate low-pass filters (LPF's). In these prototype designs, two impedance-matching schemes are proposed to optimize the embedding impedance presented to the mixer element. One scheme employs a simple quarter-wavelength impedance transformer while an alternative approach utilizes two d-HEB's fabricated in series at the feed-point of the annular slot. To reduce the footprint of the circuit and permit high packing density, a compact LPF design that significantly reduces circuit size is introduced. DC test results, including R-T and I-V measurements, indicate successful fabrication of the d-HEB's. A quasi-optical mixer block has been fabricated for RF measurements. Preliminary measurements of conversion gain, coupling efficiency, and noise temperature are presented and demonstrate promising performance of these single-element HEB mixers for imaging array applications.

Index Terms—Hot-electron bolometer, heterodyne receiver, annular slot antenna, imaging array.

Fig. 1. Measured and simulated second harmonic conversion loss versus the number of diode pairs.

I. INTRODUCTION

SUPERCONDUCTING hot-electron bolometers (HEB's) with high sensitivities have been a subject of great interest over the past few years for submillimeter receivers in radio astronomy [1][2][3]. These devices are especially attractive for frequencies above the superconducting gap of niobium superconductor-insulator-superconductor (SIS) receivers ($\sim$ 700 GHz). Compared to phonon-cooled HEB's, *diffusion-cooled* HEB's (d-HEB's) have shorter device lengths ($L < L_{e-ph}$, where L_{e-ph} is the mean free path for inelastic electron-phonon scattering), which allow hot electrons to out-diffuse to contact pads before scattering to the substrate. Due to the superconducting d-HEB's merits (i.e., broad IF bandwidth, low noise temperature and high sensitivity), single element receivers and mixers employing these devices have been proposed and studied by a variety of research groups [4][5][6]. However, few of the RF circuit designs utilized in these receivers have been suitable for imaging arrays — an application that can reduce observing and processing time by recording imaging information in parallel. The slot-ring antenna (SRA) provides a compact and attractive structure for this application, making it an ideal candidate for high resolution imaging arrays (see fig. 1) [7][8].

In this paper, the design of a quasi-optical single-element mixer operating at 585 GHz is presented that consists of a SRA and superconducting d-HEB integrated on a single silicon chip. The fabrication process employs electron-beam lithography (EBL). DC test results are presented in this paper as well as RF measurements and characterization.

II. MIXER DESIGN

Gerecht *et al*, first developed a SRA coupled HEB mixer based on NbN phonon-cooled microbridges [9][10]. For the mixer described in this paper, two impedance-matching schemes are proposed to optimize power coupling from the SRA's to the mixer elements. One scheme employs a simple quarter-wavelength impedance transformer while the alternative approach utilizes two d-HEB's fabricated in series at the feed-point of the SRA. The aspect ratio of the HEB's are chosen to present an optimum impedance to the antenna, while keeping an upper limit on the individual device lengths that is less that the mean freee path for inelastic electron-phonon scattering (L_{e-ph}). Silicon is chosen as the mixer substrate because of its relatively high dielectric constant ($\epsilon_r = 11.7$), which results in high directivity and efficiency for the receiving antenna [12][14]. The SRA is designed to operate at 585 GHz and has a radius, a, of 36 μm and a slot width, 2w, of 2.6 μm.

ADS momentum simulations of the slot-ring antenna performance is shown in Fig. 2. The designed SRA has a 3-dB bandwidth of approximately 100 GHz (16%). At 585 GHz, the real and imaginary parts of the antenna input impedance
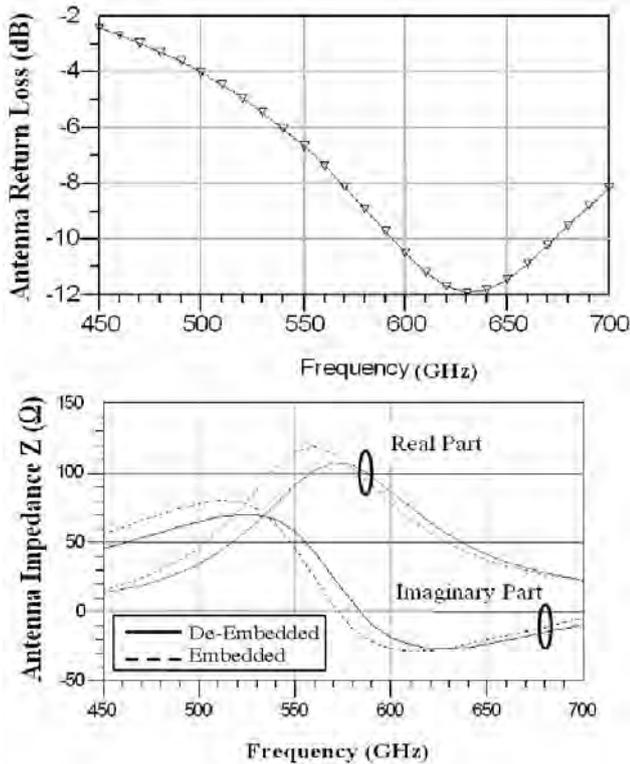
Fig. 2. Measured and simulated second harmonic conversion loss versus the number of diode pairs.

Fig. 3. Circuit model of one section of the distributed balanced doubler. Z_{Slotline} and Z_{CPW} are the unloaded slotline and CPW transmission line impedances respectively, and ℓ is the spacing between the diode pairs. Series resistance, junction capacitance and other lumped elements associated with the varactor (including parasitic bondwire inductance) are included in the diode model.

are 100 Ω and approximately zero, respectively. Consequently, impedance matching to the devices is relatively straightforward because the superconducting HEB bridge is expected to be a purely resistive device. A d-HEB with resistance as high as 100 Ω, however, requires nearly 3 squares of Nb thin film (10 nm thick with a sheet resistance of 35 Ω/square in the normal state). Hence, the resulting device length approaches that of the inelastic electron-phonon mean free path, $L_{\text{e-ph}}$. Because the resolution of the Nanometer Pattern Generation System (NPGS) employed at the University of Virginia is approximately 100 nm, the resulting device could well exceed the maximum length for diffusion cooling. As a result, two different schemes are proposed to match the 100 Ω antenna impedance to the HEB bridge in the mixer design. The first scheme employs a simple quarter-wavelength impedance transformer (scheme-I) while the second utilizes two HEB microbridges fabricated in series (each with a normal-state resistance of 50 Ω) and connected by a gold cooling pad (scheme-II).

Conventional high/low stepped-impedance low-pass filters (LPF's) are typically used for mixer circuits because they are simple to design and implement. For high insertion loss in the stopband, many stages are normally used, thus increasing size of the overall circuit. In the present design, a compact LPF is introduced that significantly reduces circuit size [11]. Fig. 3 shows the s-parameters (simulated with ADS Momentum) of a conventional 5-step LPF (258 μm in length) and one-cell of the compact LPF structure (108 μm in length). In the compact LPF, the RF signal at 585 GHz is suppressed by 30 dB while

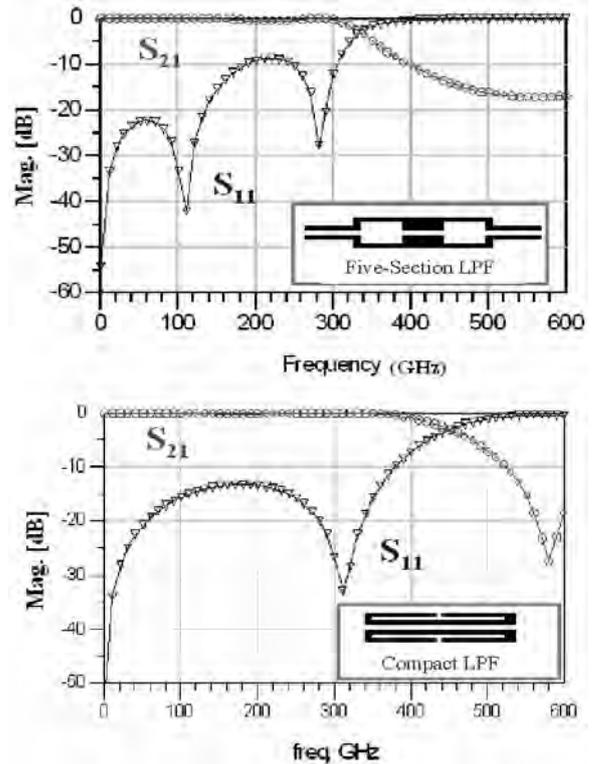the overall circuit length is reduced by 55% (from 330 μm to 180 μm). Moreover, the compact LPF can be placed anywhere in the IF output circuits, which permits flexibility in design.

Fig. 5(a) shows a diagram of a quasi-optical HEB mixer mounted on an extended hemispherical silicon lens with radius $R = 4.5$ mm. The lens focuses incident radiation onto the SRA. Radiation patterns of the SRA on silicon lens are calculated using the ray-tracing technique of Filipovic [14]. Shown in Fig. 3(b) are the E-plane patterns for various extension lengths. An extension length of 1600 μm is chosen to achieve the highest antenna directivity while keeping an acceptable Gaussian coupling efficiency [14].

III. FABRICATION

The HEB fabrication used in this work is based on a process developed by the University of Virginia's Superconducting Device and Materials Research Group [15]. The process begins with sputtering of a niobium/gold (10 nm/10 nm) bi-layer onto a Si wafer, followed by a standard lift-off process to define the base layer. The base layer consists of the slot-ring antenna, lowpass filter and tuning circuits. These are based on coplanar waveguide with a 200 nm thick Au layer.

After the base layer is defined, the mixing element - the HEB bridge - is fabricated using a two-step electron-beam lithography (EBL) process. In the first step, a bilayer PMMA (950/495) is spun on the base layer as the resist structure. The

-HEB cooling pads patterns are then directly written by an electron-beam controlled by the NPGS. The trilayer Nb/Au/Nb (10 nm/50 nm/10 nm) cooling pads are hence generated and the Nb microbridge length is defined after a lift-off process. During the second EBL step, the HEB bridge is first patterned by the NPGS. A Au/Nb (20 nm/20 nm) bilayer is deposited, and after lift-off, a bridge is left spanning the cooling pads.

Reactive-ion etches (RIE) are then performed to remove the unwanted metal layers, leaving a Nb bridge between the gold cooling pads. The length of the HEB bridge is chosen to be approximately 200 nm, a value well below the inelastic electron-phonon scattering length, resulting in a diffusion-cooled HEB device. The bridge width can be modified to produce the desired device resistance for circuit matching since the sheet resistance for 10 nm thick Nb film is known to be 35 Ω/square in the normal state [15].

Fig. 5 shows typical fabrication results for the scheme-I and scheme-II mixer circuits. In fig. 5(a), the one-square HEB bridge (HEB-A1-4) is fabricated at the end of the quarter-wave transformer with a device length of 240 nm and a device width of 237 nm, resulting in a device resistance of 35 Ω. In 5(b), the HEB bridge width is designed to be 175 nm, and the lengths of the two series HEB bridges are equal to be 250 nm. However, the measurement shows that in the mixer in fig. 5(b) (HEB-B1-4), the left-hand side HEB length is 266 nm and the right-hand side one is 230 nm. Additional measurements have demonstrated that this is not an exceptional case, but a common phenomenon with our fabrication process. This is attributable to the displacement of the alignment markers and the e-beam writing position. Because the IF bandwidth of the mixer will be determined by the longer HEB bridge ($f_{3\text{ dB}} = \pi D/2L^2$) [16], two identical series HEB bridges with equal device lengths are preferred to achieve impedance matching while maximizing the IF bandwidth.

IV. MEASUREMENTS

Room temperature probe station measurements show the resistance of the one-square Nb microbridge in Fig. 5 a is approximately 70 Ω (with the RF circuit and transformer contributing approximately 20 Ω). This result agrees with theoretical predictions, once the residual resistance ratio (RRR ~ 2 in our case) of thin Nb film is taken into account. To further explore the superconducting properties of the Nb film HEB, R-T curve measurements of the mixer HEB-A1-4 are performed and shown in Fig. 6(a). A sharp resistance transition from the superconducting state to the normal state is observed at a critical temperature $T_c = 5.4$ K with a transition width $\Delta T_c \sim 0.5$ K. Shown in Fig. 6(b) is the low temperature I-V curve of this device measured at 4.7 K. The critical current is around 120 μA, corresponding to a $J_c \sim 5.1 \times 10^6$ A/cm^2, comparable to the results reported by other groups. The normal state resistance is 29 Ω, implying a thicker-than-designed Nb thin film has been fabricated, resulting in a smaller-than-expected sheet resistance.

The IF output consists of a coplanar transmission line fabricated on a Si wafer with a thickness of 1.1 mm. This results in a total lens-supported antenna extension length
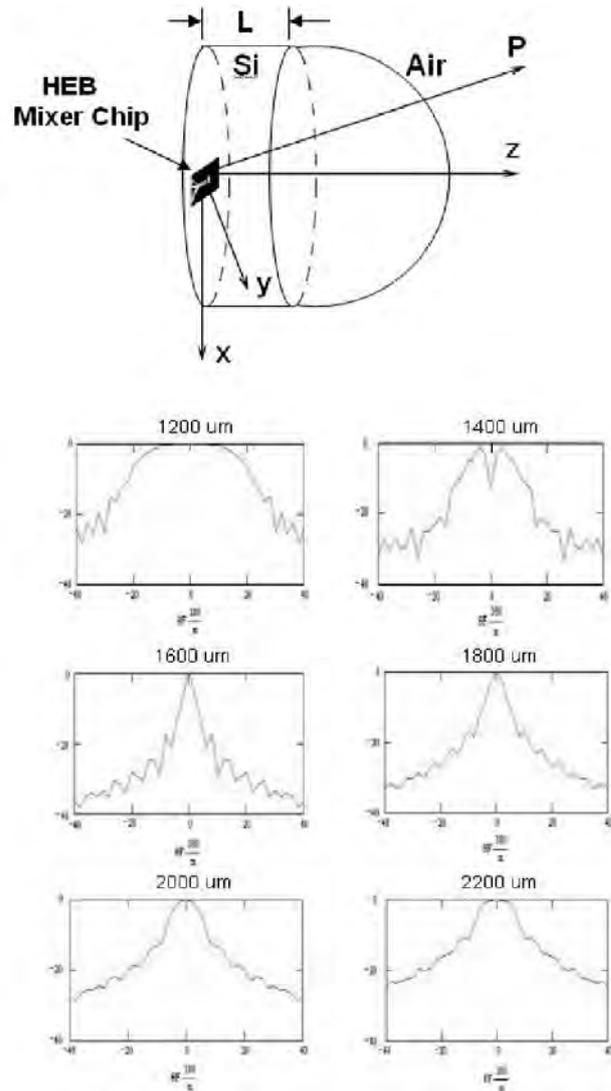

Fig. 4. Measured and simulated second harmonic conversion loss versus the number of diode pairs.

of approximately 1.6 mm. A quasi-optical mixer block to support the IF substrate/HEB chip is fabricated from brass and installed into an HD-3(8) dewer system for cryogenic testing and RF measurements. Fig. 7 shows the diagram of the RF measurement system used to measure the mixer parameters including conversion gain, coupling efficiency, and noise temperature. In this system, a VDI 576–640 GHz Frequency Extension Module (courtesy of Virginia Diodes, Inc.) is employed to provide the LO power. A hot/cold load is used to measure the system Y-factor. Both the LO and RF are coupled into the cryogenic dewar through a set of lenses and mirrors. Inside the dewar, the quasi-optical mixer block is placed before a teflon window and biased from a bias-T. The IF signal is output to an isolator and low noise amplifier (LNA) before being fed to an external (room temperature) IF chain for data processing.

Prior to performing the Y-factor measurement, pumped I-V curves at 585 GHz (Fig. 8) are measured by coupling into the dewar the LO signal. As expected, the critical current
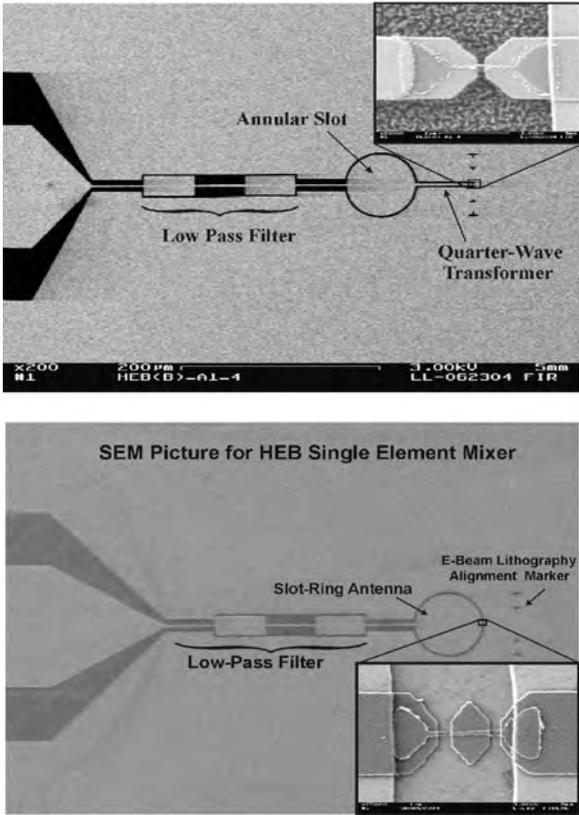
Fig. 5.   Measured and simulated second harmonic conversion loss versus input frequency for 6 diode pairs.

Fig. 6.   Measured and simulated second harmonic conversion loss versus input frequency for 6 diode pairs.

decreases with increasing LO power. The HEB device is saturated (i.e., behaves as a pure resistance) at a LO power of P4, indicating the entire Nb microbridge is pumped from the superconducting state into the normal state.

The frequency response of the system is measured with an amplitude-chopped LO. The response of the HEB is maximum at 600 GHz and a second maximum occurs at 615 GHz. These are likely attributable to the transmission characteristic of the mesh-filter and the frequency response of the SRA, respectively. These peaks are slightly shifted from their designed values. The measured E-plane radiation pattern of the SRA-coupled HEB is shown in Fig. 9 and the main beam demonstrates good agreement with calculation.

V. DISCUSSION

In this paper, a SRA-coupled 585 GHz d-HEB mixer for imaging array applications has been designed and fabricated. To optimize the power coupling from the SRA to the mixing element, two impedance matching schemes have been proposed. A compact LPF structure has been introduced to provide for a more compact mixer for future imaging array applications.

DC and RF measurements demonstrated the successful design and fabrication of the SRA-coupled d-HEB mixer. The parameters at 585 GHz including coupling efficiency, noise temperature and conversion gain will soon be fully investigated for evaluation of the mixer performance. Future work also includes investigation of mutual coupling between adjacent
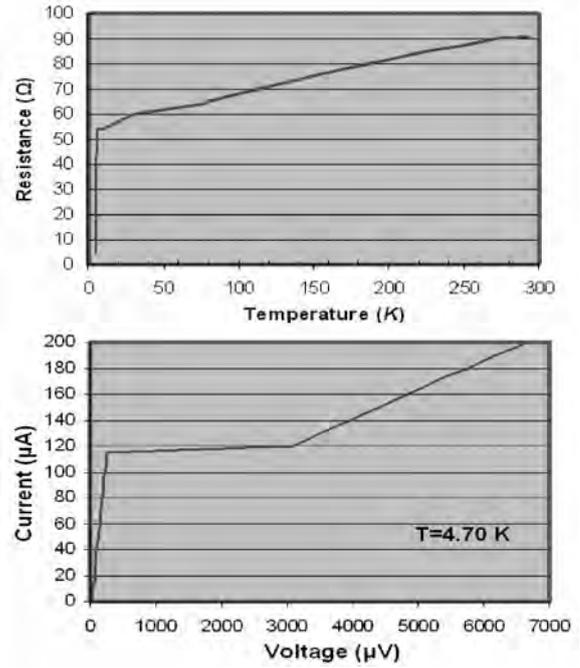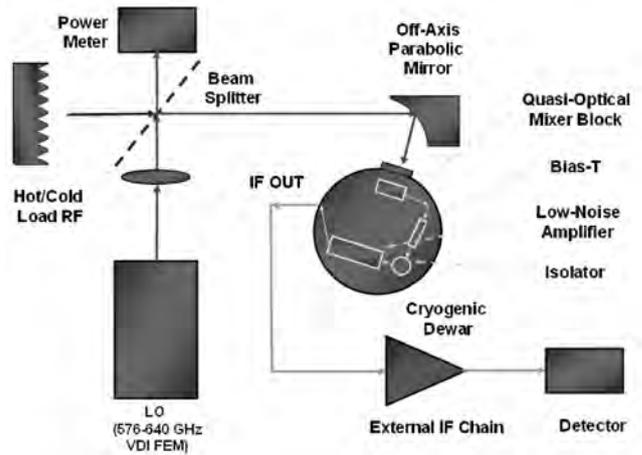

Fig. 7.   Measured P_{in} v. P_{out} at the fundamental, second, and third harmonics for the distributed balanced doubler. The input power is 27 dBm (500 mW) and the peak output power at the second harmonic is 22.6 dBm (180 mW)

SRA's and expansion of the single HEB mixer to a full imaging array.

REFERENCES

[1] D. E. Prober, "Superconducting terahertz mixer using a transition-edge microbolometer," *Appl. Phys. Lett.*, vol. 62, pp. 2119-2121, 1993.
[2] H. Ekström, B.S. Karasik, E.L. Kollberg, and K.S. Yngvesson, "Conversion gain and noise of Niobium superconducting hot-electron-mixers," *IEEE Trans. Microwave Theory Tech.*, vol. 43, no. 4, pp. 938-947, Apr. 1995.
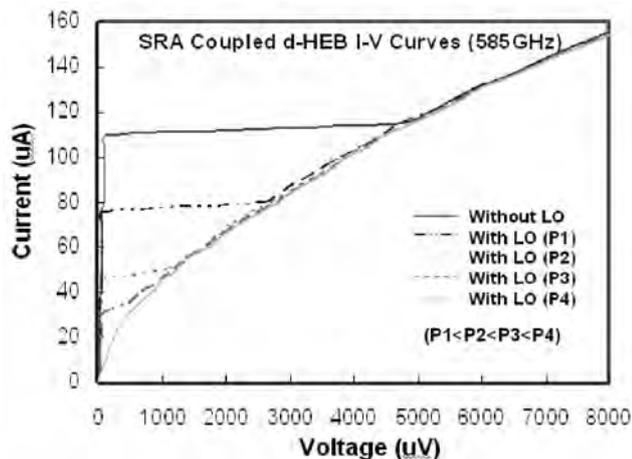
Fig. 8. Measured P_{in} v. P_{out} at the fundamental, second, and third harmonics for the distributed balanced doubler. The input power is 27 dBm (500 mW) and the peak output power at the second harmonic is 22.6 dBm (180 mW)

Fig. 9. Measured P_{in} v. P_{out} at the fundamental, second, and third harmonics for the distributed balanced doubler. The input power is 27 dBm (500 mW) and the peak output power at the second harmonic is 22.6 dBm (180 mW)
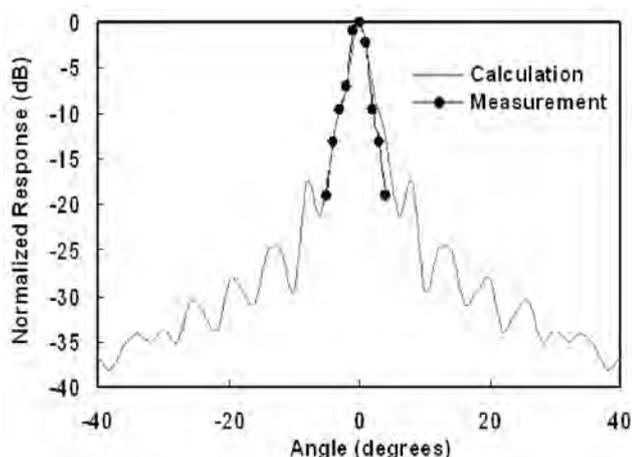
[10] F. Rodriguez-Morales, K.S. Yngvesson, E. Gerecht, N. Wadefalk, J. Nicholson, D. Gu, X. Zhao, T. Goyette, and J. Waldman, "A terahertz focal plane array using HEB superconducting mixers and MMIC IF amplifiers," *IEEE Microwave and Wireless Comp. Lett.*, vol. 15, no. 4, pp. 199–201, April 2005.

[11] J. Sor, Y. Qian, and T. Itoh, "Miniature low-loss CPW periodic structures for filter applications," *IEEE Trans. Microwave Theory Tech.*, vol. 49, no. 12, pp. 2336-2341, Dec. 2001.

[12] D.B. Rutledge, D.P. Neikirk, and D.P. Kasilingam, "Integrated-circuit antennas," *Infrared and Millimeter Waves,*, vol. 10, Chap. 1, Academic Press Inc. 1979.

[13] R. E. Collin, *Antennas and Radiowave Propagation* New York McGraw-Hill, ch.4, 1985.

[14] D.F. Filipovic, S.S. Gearhart, and G.M. Rebeiz, "Double-slot antennas on extended hemispherical and elliptical silicon dielectric lenses," *IEEE Trans. Microwave Theory Tech.*, vol. 41, no. 10, Oct. 1993.

[15] R. B. Bass, "Hot-electron bolometers on ultra-thin silicon chips with beam leads for a 585 GHz receiver," Ph.D. dissertation, University of Virginia, May 2004.,

[16] I. Siddiqi, A. Verevkin, D.E. Prober, A. Skalare, B.S. Karasik, W.R. McGrath, P. Echternach, and H. G. LeDuc,, "Noise and conversion efficieny of Aluminum superconducting hot-electron bolometer mixer," *IEEE Trans. Appl. Supercon.*, vol. 11, no. 1, March 2001.

[3] B. S. Karasik and A. I. Elantiev, "Noise temperature limit of a superconducting hot-electron bolometer mixer," *Appl. Phys. Lett.*, 68 (6), Feb. 1996.

[4] A. Skalare, W. R. McGrath, B. Bumble, H.G. LeDuc, "Receiver measurements at 1267 GHz using a diffusion-cooled superconducting transition-edge bolometer," *IEEE Trans. Appl. Supercon.*, vol. 7, no. 2, June 1997.

[5] W. F. M. Ganzevles, L. R. Swart, J. R. Gao, P. A. J. de Korte, T. M. Klapwijk, "Direct response of twin-slot antenna-coupled hot-electron bolometer mixers desined for 2.5 THz radiation detection," *Appl. Phys. Lett.*, vol. 76, no. 22, May 2000.

[6] W. F. M. Ganzevles, J. R. Gao, D. Wilms Floet, G. de Lange, A. K. van Langen, L.R. Swart, T.M. Klapwijk, and P. A. J. de Korte, "Twin-slot antenna coupled Nb hot electron bolometer mixers at 1 THz and 2.5 THz," *Proc. 10th Int. Symp. On Space Terahertz Technology*, University of Virginia, Charlottesville, USA, March 16-18, 1999, pp. 246.

[7] C.E. Tong, and R. Blundell, "An annular slot antenna on a dielectric half-space," *IEEE Trans. Antennas and Propagation*, vol. 42, no. 7, pp. 967-974, July 1994.

[8] S. Raman and G.M. Rebeiz, "Single- and dual-polarized millimeter-wave slot-ring antennas," *IEEE Trans. Antennas Propagat.*, vol. 44, no. 11, pp. 1438-1444, Nov. 1996.

[9] E. Gerecht, D. Gu, X. Zhao, J. Nicholson, F. Rodriguez-Morales, and K.S. Yngvesson, "Development of NbN terahertz HEB mixers coupled through slot-ring antennas," *Proc. 15th Int. Symp. On Space Terahertz Technology*,University of Massachusetts, Amherst, 2004.